

A highly reliable 32-channel wavelength division demultiplexer (patent pending)^a

James W. Horwitz, Xuegong Deng*, Al Morgan**, Jie Qiao*, Victor Villavicencio, Feng Zhao*, Jizuo Zou*, Ray T. Chen*

Radiant Research, Inc., 3006 Longhorn Boulevard, Suite 105, Austin, Texas 78758

*Microelectronics Research Center, Department of Electrical and Computer Engineering
University of Texas at Austin, Austin, Texas

**Al Morgan and Associates, Austin, Texas

ABSTRACT

A 32-channel wavelength-division demultiplexer (WDDM) has been designed and tested. Intended for commercial use, the instrument is designed to be rugged, stable, and insensitive to temperature variations. Operating in the 1.54- to 1.57- μm spectral range, the unit uses single-mode fiber input and multi-mode fiber output. The optics consists of a Littrow plane-grating spectrograph that uses the same lens for collimation and for focusing. In order to reduce the size of the device, the grating is used at a large diffraction angle. A coarse ruling is used in a high diffraction order, which results in a device that has a low polarization-dependent loss. The mean insertion loss for all channels was 3.1 dB, and the standard deviation of the insertion loss was 0.23 dB. The mean channel bandwidth was 0.26 dB.

Keywords: Wavelength division multiplexing, WDM, gratings, spectrographs, fiber optics

1. INTRODUCTION

Wavelength-division multiplexers (WDMs) have come into widespread use in optical communication networks. We illustrate the basic concept of such devices in Fig. 1. Near-infrared optical signals are generated by lasers or LEDs at a series of monochromatic wavelengths $\lambda_1, \lambda_2, \dots, \lambda_n$ and sent through n fibers to a WDM. These signals are combined by the WDM into a polychromatic signal, which is launched into a single fiber. This multiplexing allows one to utilize the very large signal bandwidth available in an optical fiber.

At the destination, a wavelength-division demultiplexer (WDDM) separates the polychromatic signals into a series of narrow-band channels. The channels have center wavelengths that are the same as the original wavelengths. The channels have spectral widths (passbands) $\Delta\lambda_i$ that are large enough to accommodate system tolerances, but small enough to avoid overlapping of the channels. In ordinary practice, neither the WDM nor the WDDM is tunable, so that these devices are basically spectrographs using fibers for input and output.

The vacuum wavelength λ and frequency ν of a wave are related by the equation

$$\frac{c}{n} = \nu\lambda, \quad (1)$$

^a This work was presented as an invited paper at S. P. I. E.'s Photonics West Conference, January 22-28, 2000, in San Jose, California (Paper No. 3949-11). As printed in the conference announcement and program, there were errors in the spelling of the authors' names and their affiliations. These errors have now been corrected. All correspondence should be directed to the first-named author (e-mail: Horwitz@RadiantR.Com).

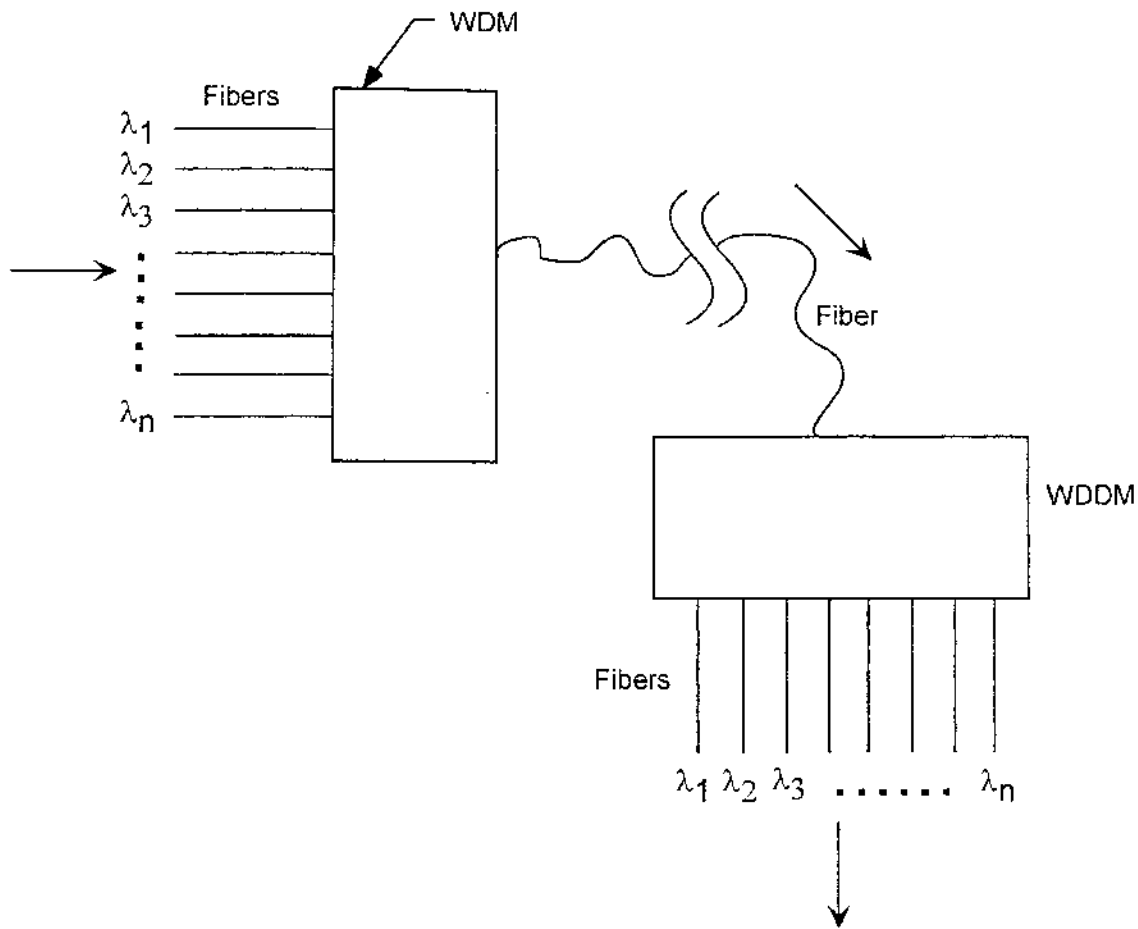
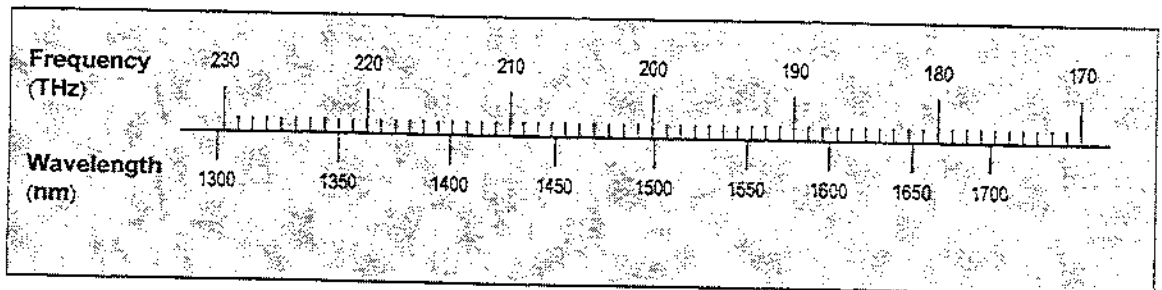


Fig. 1. The WDM/WDDM concept.

where n is the refractive index of the medium in which the wave travels and c is the speed of light in a vacuum.

In fiber-optic communication, the frequency is used to define the wave parameters rather than the wavelength. Therefore, the International Telecommunications Union (ITU) has adopted a standard for optical communication that specifies that certain standard frequencies be used to identify and specify WDM channels. Figure 2 illustrates the relationship between frequency and wavelength given by (1), assuming that $n = 1$. The standard ITU frequencies are at multiples and sub-multiples of 100 GHz. For instance, 193.1 THz = 193 100 GHz is an ITU standard frequency, because it is a multiple of 100 GHz. A WDM is said to operate on the 100-GHz ITU grid if its channel frequencies are spaced at 100-GHz intervals. Similarly, there is a 200-GHz grid and a 50-GHz grid.

Using (1) and $c = 2.99792458 \times 10^8$ m/s, we see that a wave at a frequency of 193.1 THz has a vacuum wavelength of 1552.524 nm. The next channel on the 100 GHz grid has a frequency of 193.2 THz and a vacuum wavelength of 1551.721 nm. Thus, the channels are about 0.80 nm apart at these frequencies.



WDM channels in frequency (THz) and wavelength (nm) in the spectrum defined by ITU-T

Fig. 2. A nomogram useful for converting between frequency and wavelength in the 1300- to 1700-nm region.

2. THE WDDM AND ITS CHARACTERISTICS

We have developed a 32-channel WDDM that operates in the 1.54- to 1.57- μm spectral range. Its nominal channel spacing is 100 GHz. This device is intended for commercial use, and our group has developed other WDDMs that use similar design principles. Fig. 3 is a photograph of the completed instrument.

The present device is a prototype, and uses a single-mode fiber for input and 32 multi-mode fibers for output. The core diameter of the single-mode fiber is 9.6 μm , and that of the multi-mode fibers is 62.5 μm . Other versions are possible with different types of fibers for input and output. As in the example above, the nominal channel spacing was about 0.8 nm. In the prototype design, due to the nonlinear nature of the grating equation, the spacing between individual channels varies from 0.75 nm at the two longest-wavelength channels to 0.85 nm at the two shortest-wavelength channels. This design uses a linear spacing of the output fibers, and its channels do not fall on the ITU grid. We have designed an alternate version that has its channels on the ITU grid. The latter version uses a nonlinear spacing of the output fibers.

The measured 1-dB channel bandwidths $\Delta\lambda_c$ of the prototype device ranged from 0.22 to 0.31 nm, with a mean value of 0.26 nm. The measured insertion loss as a function of channel number is shown in Fig. 4. The mean value of the insertion loss was 3.1 dB, and its standard deviation was 0.23 dB. Also of interest is the cross talk

between adjacent channels. Although we do not report a measured value here, we expect that production versions of this instrument will have cross talk that does not exceed -25 dB.

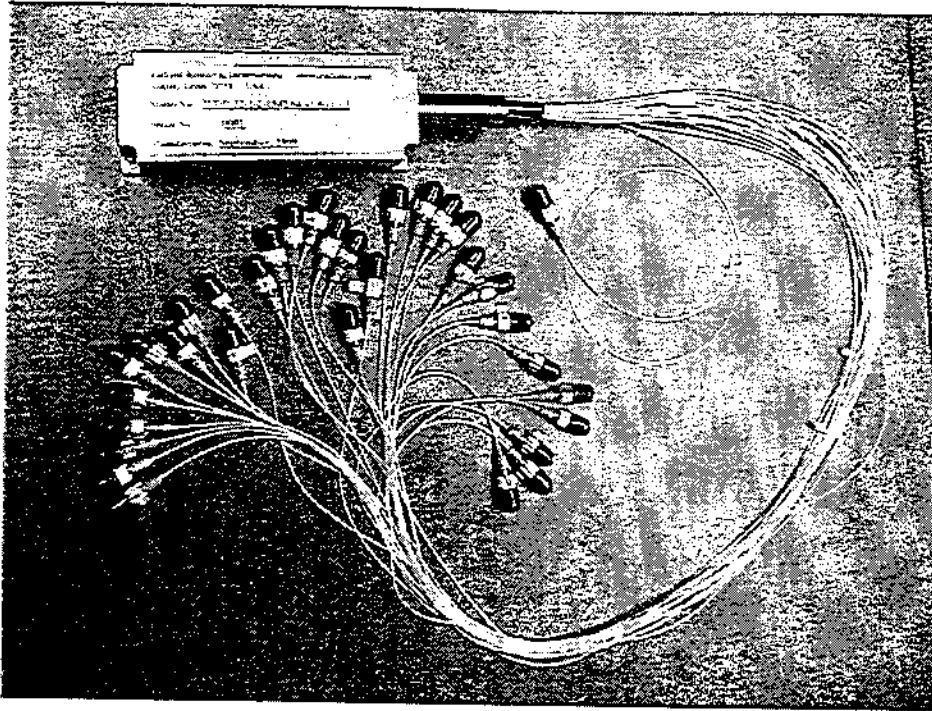


Fig. 3. The 32-channel WDDM. The instrument is 6.3 in. long, 2.3 in. wide and 1.8 in. high. The input fiber is coiled for this photograph, while the 32 output fibers are bunched together and are not coiled.

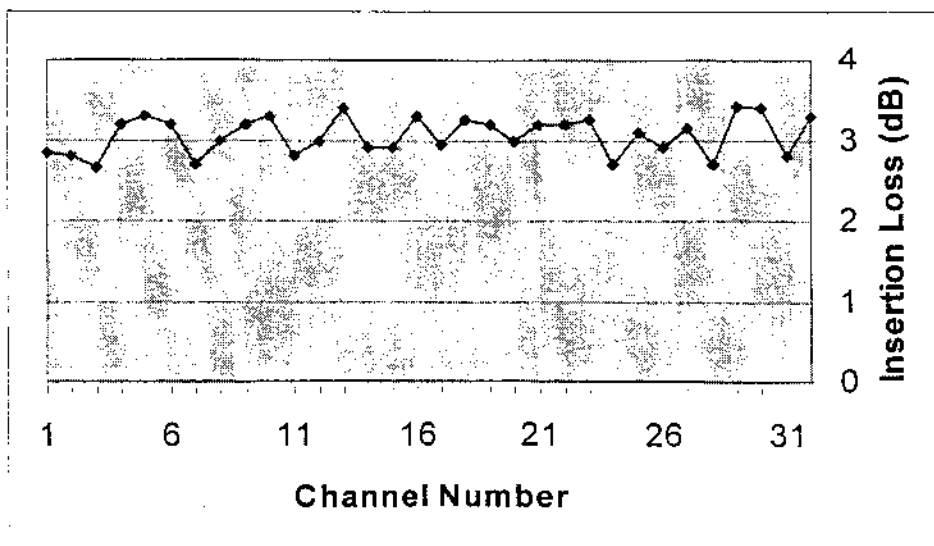


Fig. 4. The insertion loss of the 32-channel WDDM as a function of channel number.

Consider a beam of wavelength λ that is focused upon an output fiber. It is of interest to know what effect a lateral misalignment will have. We purposely shifted the beam laterally until the insertion loss increased by 1.0 dB. The shift needed was 25 μm , which is 40 percent of the core diameter of an output fiber. This shift was equivalent to a 0.09 nm change in wavelength.

We have analyzed in detail the theoretical temperature sensitivity of instruments like ours. Although we are not ready to publish our calculations yet, our analysis shows that, with careful design, the effects of isothermal temperature changes on the channel wavelengths can be made negligible, while the variation of insertion loss with temperature can be made acceptably small. Our analysis used an operating temperature range of -5°C to $+60^\circ\text{C}$. In Section 4 below, we show the result of thermal testing of a device similar to ours.

3. OPTICAL DESIGN OF THE WDDM

A simplified diagram of the optics of the WDDM is shown in Fig. 5 (a). Light from the input fiber (not shown) illuminates the lens, which collimates the light. The collimated beam strikes a diffraction grating, which has been tilted at an angle θ . The grating disperses the light into its wavelengths, and the dispersed beam passes through the lens a second time. For simplicity, the dispersion is omitted from the diagram. The lens focuses the light for each channel onto a separate output fiber (not shown). Like the input fiber, the output fibers are located in the focal plane of the lens. This arrangement forms a Littrow spectrograph, and the grating angle is related to the grating spatial frequency f and the wavelength λ by the equation

$$2 \sin \theta = \frac{m\lambda f}{n}, \quad m = 0, \pm 1, \pm 2, \dots, \quad (2)$$

where m is an integer called the order of diffraction and n is the index of refraction of the medium containing the incident and diffracted rays [see Fig. 5(b)]. This equation assumes that the input fiber and output fiber for the wavelength of interest both lie on the optical axis of the lens, which is usually only an approximation to the actual design conditions.

Equation (2) is a special case of the two-dimensional grating equation

$$\sin \alpha + \sin \beta = \frac{m\lambda f}{n}, \quad (3)$$

where α is the angle of incidence and β is the angle of diffraction, as shown in Fig. 5(b). This equation applies when both incident and diffracted rays lie in the plane of the diagram, and it allows one to find the direction of a diffracted ray once the direction of the incident ray is known. Taking the partial derivative of (3) with respect to λ and holding α constant, we have

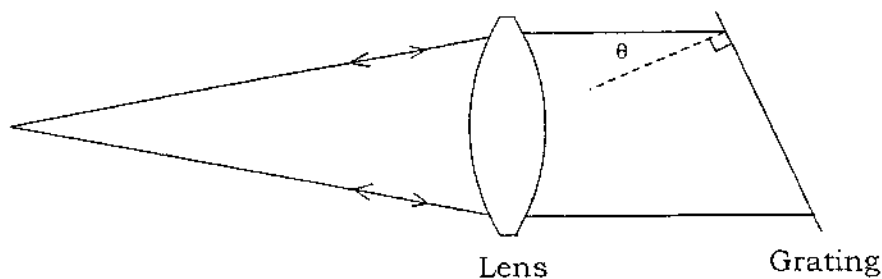
$$\frac{\partial \beta}{\partial \lambda} = \frac{mf}{n \cos \beta}. \quad (4)$$

If we make the assumption that the lens is aberration-free, then the laws of paraxial lens optics apply. The use of these laws in conjunction with (4) allows one to compute the focal length F of the lens once the fiber spacing Δy and wavelength increment $\Delta \lambda$ between adjacent channels is known. The result is

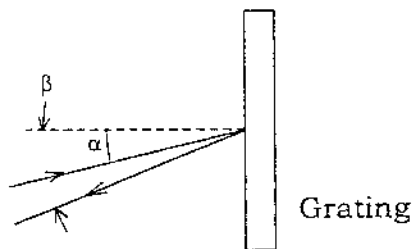
$$F = \frac{\Delta y}{\Delta \lambda} \frac{n \cos \beta}{mf}. \quad (5)$$

This formula shows that the focal length of the lens is directly proportional to the fiber spacing and to the cosine of the angle of diffraction. Since $\beta \approx \theta$, the lens focal length is also directly proportional to $\cos \theta$, the cosine of the grating angle. Thus, in order to make the lens small, one uses closely spaced fibers and a large grating angle. However, if θ exceeds about 25° , the space taken up by the grating begins to increase, so that the overall size of the instrument is not reduced in proportion to the size of the lens.

We designed the lens to have optimum performance for the present application. By considering the aberrations of the optical system as a whole, we were able to make an accurate prediction of the optical performance of our WDDM prior to building it.



(a)



(b)

Fig. 5. (a) A simplified schematic of a WDDM. (b) Definition of the angles of incidence and diffraction.

4. THERMAL TESTING OF A HOLOGRAM-TYPE WDDM

Our group previously developed a four-channel wide-bandwidth WDDM that operates in the vicinity of 810 nm. This instrument uses a holographic transmission grating that was produced by us, and it has two separate lenses to achieve collimation and focusing. It has a photopolymer volume hologram grating that is attached to a BK7 glass substrate. The thermal expansion of the grating is probably dominated by the BK7. See Fig. 6.

The thermal performance of this instrument is shown in Figs. 7 and 8. The thermal wavelength shifts shown in these plots, although small (0.08 nm maximum), would not be negligible in a narrow-band (dense) device like our 32-channel instrument. However, we plan to incorporate certain design features in production versions of the 32-channel device in order to reduce the thermal shifts in wavelength to very small values. The insertion loss variation of the four-channel instrument as a function of temperature is, as seen in Fig. 8, quite small (less than ± 0.02 dB).

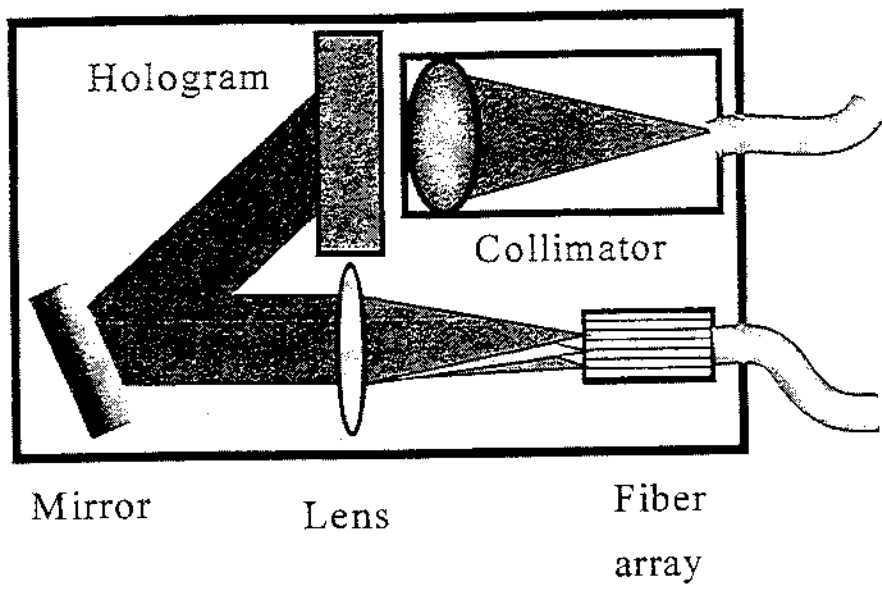


Fig. 6. A four-channel wide-band WDDM developed by our group.

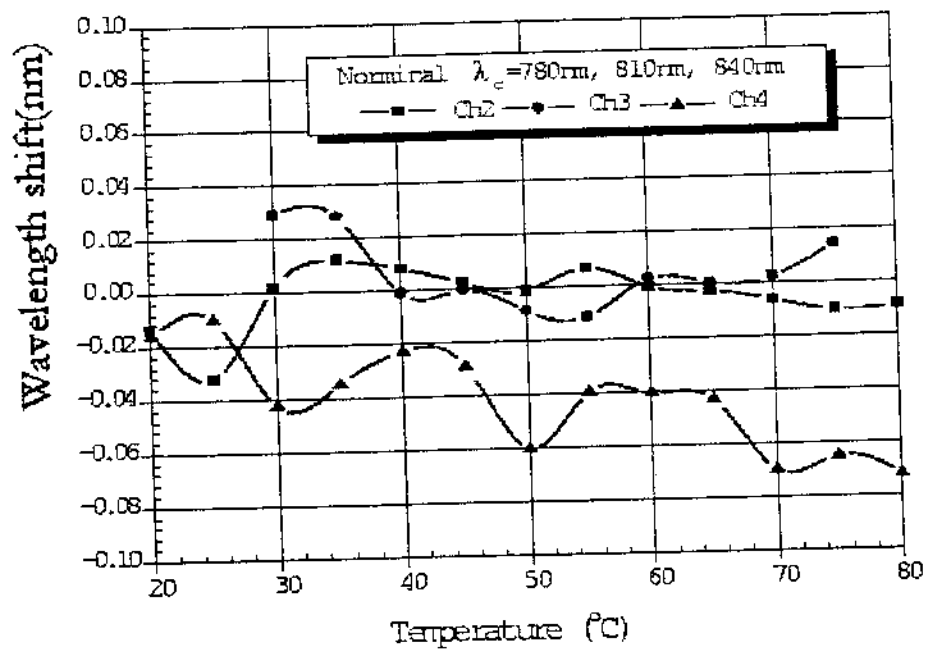


Fig. 7. Wavelength shift of three channels of the four-channel WDDM as a function of temperature.

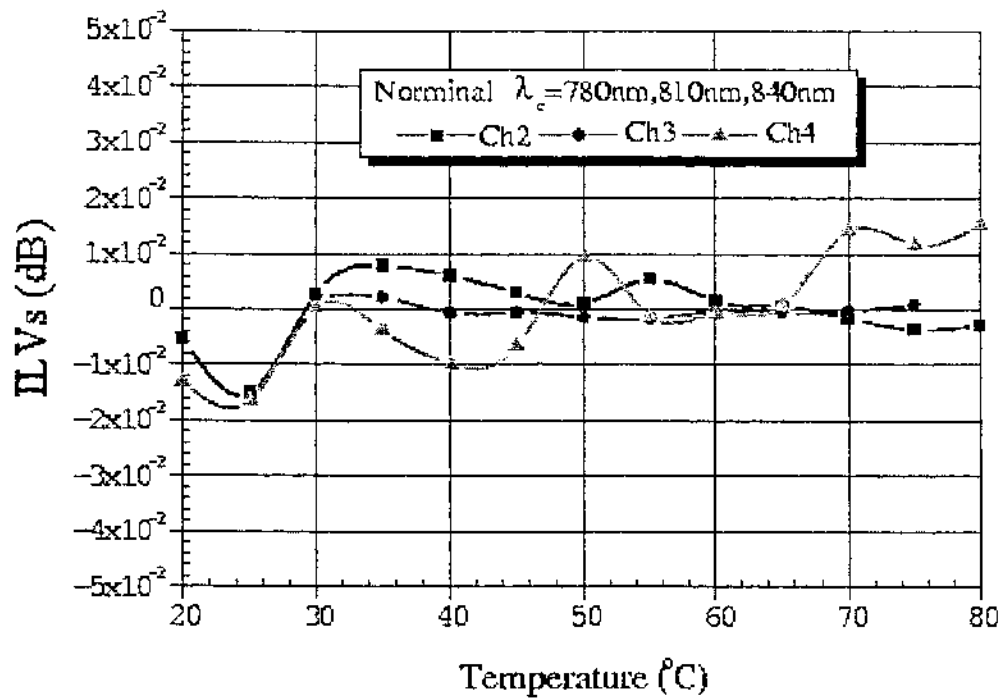


Fig. 8. The variation of insertion loss (ILV) of three channels of the four-channel WDDM as a function of temperature.

5. REFERENCES

1. R. C. Weast, ed., *CRC Handbook of Chemistry and Physics*, 64th ed. (CRC Press, Boca Raton, Fla., 1985), p. F-198.